


Please cite the Published Version

Doyle, AM , Albayati, TM, Abbas, AS and Alismaeel, ZT (2016) Biodiesel production by esterification of oleic acid over zeolite Y prepared from kaolin. *Renewable Energy*, 97. pp. 19-23. ISSN 0960-1481

DOI: <https://doi.org/10.1016/j.renene.2016.05.067>

Publisher: Elsevier

Version: Accepted Version

Downloaded from: <https://e-space.mmu.ac.uk/637/>

Usage rights:  [Creative Commons: Attribution-Noncommercial-No Derivative Works 4.0](https://creativecommons.org/licenses/by-nc-nd/4.0/)

Additional Information: This is an Author Accepted Manuscript of a paper accepted for publication in *Renewable Energy*, published by and copyright Elsevier.

Enquiries:

If you have questions about this document, contact openresearch@mmu.ac.uk. Please include the URL of the record in e-space. If you believe that your, or a third party's rights have been compromised through this document please see our Take Down policy (available from <https://www.mmu.ac.uk/library/using-the-library/policies-and-guidelines>)

1 **Biodiesel production by esterification of oleic acid over zeolite Y prepared from kaolin**

2 **Aidan M. Doyle^{1*} Talib M. Albayati^{2*} Ammar S. Abbas³ Ziad T. Alismaeel⁴**

3 1. Division of Chemistry and Environmental Science, Manchester Metropolitan University, Chester St.,
4 Manchester, M1 5GD, United Kingdom. email: a.m.doyle@mmu.ac.uk

5
6 2. Department of Chemical Engineering, University of Technology, 52 Alsinaa St., PO Box 35010,
7 Baghdad, Iraq. email: talib_albyati@yahoo.com.

8
9 3. Department of Chemical Engineering, College of Engineering, University of Baghdad, Al-Jadryah, P.O.
10 Box 47221, Baghdad, Iraq. email: dr_ammarr19@yahoo.com.

11
12 4. Department of Biochemical Engineering, Al-Khwarizmi College of Engineering, University of Baghdad,
13 Al-Jadryah, P.O. Box 47008, Baghdad, Iraq. email: ziadalismaeel@yahoo.com.

14
15
16 * Corresponding authors: a.m.doyle@mmu.ac.uk; talib_albyati@yahoo.com

17
18 **Abstract**

19 Zeolite Y, with a Si/Al ratio 3.1, was prepared using Iraqi kaolin and tested as a catalyst in the
20 liquid-phase esterification of oleic acid (a simulated free fatty acid frequently used as a model
21 reaction for biodiesel production). XRD confirmed the presence of the characteristic faujasite
22 structure of zeolite Y, and further analysis was conducted using BET adsorption, FTIR
23 spectroscopy, XRF, DLS particle size and SEM. A range of experimental conditions were
24 employed to study the reaction; alcohol/oleic acid molar ratio, temperature, and catalyst mass
25 loading. The optimum conditions for the reaction were observed at 70 °C, 5 wt% catalyst loading
26 and 6:1 ethanol to oleic acid molar ratio. The oleic acid conversion using the zeolite prepared from
27 kaolin was 85% after 60 min, while the corresponding value for a commercial sample of HY zeolite
28 was 76%. Our findings show that low Si/Al ratio zeolite Y is a suitable catalyst for esterification,
29 which is in contrast to the widespread view of the unsuitability of zeolites, in general, for such
30 applications.

31
32 **Keywords;** Biodiesel, esterification, Y zeolite, kaolin, Si/Al ratio.

37 **1. Introduction**

38 Biodiesel is an alternative fuel produced from natural sources such as vegetable oils and animal
39 fats [1-4]. Vegetable oils were first used as fuels over a century ago by Rudolf Diesel but this
40 source of fuel has been replaced by cheaper petroleum oil fractions that are reformed to diesel
41 using heterogeneous catalysts. Despite the continuing widespread use of fossil fuels, and recent
42 technologies that allow increasing amounts of extraction from previously unavailable sources, the
43 total amount of petroleum oil that is available is limited and will someday expire. Vegetable oils
44 are extracted from plants and are therefore an almost limitless means of storing solar energy.
45 Natural oils typically comprise mostly glycerides/triglycerides and suffer from high viscosity and
46 inappropriate burning rate (cetane number), both of which render them less than ideal as fuels for
47 transportation.

48
49 The (trans)esterification of natural oils using heterogeneous catalysis overcomes these problems
50 by generating alkyl esters that are much more suited to use as fuels, and a number of reviews have
51 been published on the use of solid-acid catalysts in such applications [5-10 and references therein].
52 However, there appears to be a general consensus in such reports that microporous zeolites are
53 unsuitable catalysts for fatty acid esterification. Some reports base this conclusion on a
54 disproportionately small number of publications whereas others mistakenly exclude the field of
55 microporous zeolites altogether. While Corma and co-workers accurately proved that pores with
56 diameter <2 nm impose a diffusion limitation for reactant molecules above a crucial dimension [
57 11] we find that certain zeolites are active in oleic acid esterification if sufficiently low Si/Al ratios
58 are employed.

59
60 Kaolin clay is a cheap and plentiful raw material found in numerous geographical locations and
61 has been used successfully in the synthesis of mesoporous aluminosilicates [12] and various
62 microporous zeolite frameworks; ZSM-5, X/Y, β , and A [13-22]. A large part of these studies was
63 the removal of impurities in the clays (typically quartz) via the thermal transformation of the
64 untreated clay into metakaolin, which is itself catalytically active in the transesterification of waste
65 cooking oil to alkyl esters [23]. The same transesterification reactions were conducted using
66 metakaolin that was transformed to zeolite A by hydrothermal activation with NaOH [24]. The
67 liquid-phase acid catalysed esterification of free fatty acids is another important reaction to

68 produce biodiesel. Li et al. reported a lanthanide ion-containing ZSM-5/MCM-41 composite
69 material, prepared from kaolin, that was active in the esterification of ethanoic acid with n-butyl
70 alcohol [25]. Da RochaFilho and co-workers investigated the esterification of oleic acid using a
71 catalyst prepared from Amazon flint kaolin, which was converted to metakaolin and subsequently
72 treated with sulphuric acid. The as-prepared materials were catalytically active but, to our
73 knowledge, no studies were reported to investigate whether the acid content is leached during
74 reaction so it is unclear how stable the catalyst is and whether the system is truly heterogeneous
75 [26-29].

76
77 Kaolin from Iraq has been used to prepare zeolite A for desulfurization of liquified petroleum gas
78 (LPG) and zeolite Y for catalytic cracking (FCC) of cumene [30-32]. Here we prepare zeolite Y
79 from Iraqi kaolin and test its catalytic activity in the liquid-phase esterification of oleic acid over
80 a range of experimental conditions; ethanol to oleic acid ratio, catalyst loading and temperature.
81 The acidic groups are generated by the charge imbalance of Al bonded to the framework of the
82 zeolite and is therefore more stable than those attached using the relatively simple loading method
83 for the Amazon flint kaolin [26-29]. Our findings demonstrate that the activity of the prepared
84 catalyst in oleic acid esterification compares favourably with that of a commercially available Y
85 zeolite.

86

87 **2. Experimental**

88 **2.1 Materials**

89 The following is a list of the materials' purity and source/supplier; kaolin clay, State Company of
90 Geological Surveying and Mining, Iraq; oleic acid ($C_{17}H_{33}COOH$), Thomas Baker; sodium
91 hydroxide (NaOH) pellets, extra pure, Scharlau; absolute ethanol (C_2H_6O), >99.8% GC, Sigma
92 Aldrich; sodium silicate (Na_4SiO_4), 99% purity, BDH Chemicals Ltd.; ammonium nitrate
93 (NH_4NO_3), Hopkin & Williams; oxalic acid dihydrate ($H_2C_2O_4 \cdot 2H_2O$), >99% purity, Fluka
94 Chemika; phenolphthalein, 2% in ethanol, Sigma-Aldrich. HY-commercial zeolite was purchased
95 from Qingdao Wish Chemicals Co. Ltd.

96

97 **2.2 Catalyst preparation**

98 Zeolite Y was prepared using the method described in Abbas and Abbas whereby NaY was first
99 prepared and then converted to HY zeolite (HY-kaolin) by ion exchange [33].

100

101 **2.3 Preparation of NaY zeolite**

102 1 part (by mass) 45-75 μm (by sieve fraction) kaolin clay was mixed with 1.5 parts (by mass) of
103 40 wt % aqueous NaOH solution and the mixture was heated at 850 $^{\circ}\text{C}$ for 3 hours in a furnace to
104 get fused kaolin. The fused kaolin was then milled to get fused kaolin in powder form. 50 g of the
105 prepared kaolin and 63 g of sodium silicate were dispersed in 500 ml of deionized water by stirring
106 at 50 $^{\circ}\text{C}$ for 1 hour giving a slurry of approximate pH 13.3. The slurry was aged at 50 $^{\circ}\text{C}$ for 24 h
107 under static conditions in a polypropylene bottle, and then crystallized at 100 $^{\circ}\text{C}$ for 48 h. The
108 solid was recovered by filtration, washed with deionized water and dried in an oven at 100 $^{\circ}\text{C}$ for
109 16 h. Finally, the dried powder was calcined in air at 500 $^{\circ}\text{C}$ for 1 h.

110

111 **2.4 Preparation of HY zeolite**

112 100 g of prepared NaY zeolite were mixed with 600 ml of 1 M ammonium nitrate at 100 $^{\circ}\text{C}$ for 4
113 h and stirred in a round bottom flask fitted with a reflux condenser. NH_4Y zeolite was recovered
114 by filtration, washed with deionized water and dried at 100 $^{\circ}\text{C}$ for 6 h. HY zeolite was prepared
115 by stirring 40 g of the prepared NH_4Y zeolite with 800 ml of 0.5 N oxalic acid at room temperature
116 for 8 h. HY zeolite was recovered by filtration, washed with deionized water, dried at 100 $^{\circ}\text{C}$ and
117 calcined in air at 550 $^{\circ}\text{C}$ for 5 h.

118

119 **2.5 Catalyst characterization**

120 X-Ray diffraction (XRD) was conducted in ambient conditions using a Panalytical X'Pert Powder
121 diffractometer with $\text{Cu K}\alpha$ radiation ($\lambda = 1.5406 \text{ \AA}$). All powder diffraction patterns were recorded
122 from 4-50 $^{\circ}$ 2θ with step size 0.026 and step time 50 s, using an X-ray tube operated at 40 kV and
123 30 mA with fixed 1/4 $^{\circ}$ anti-scatter slit. Nitrogen adsorption/desorption measurements were carried
124 out using a Micromeritics ASAP 2020 Surface Analyser where samples were degassed under
125 vacuum ($p < 10^{-5}$ mbar) for 12 h at 350 $^{\circ}\text{C}$ prior to analysis. BET-surface areas of the samples were
126 calculated in the relative pressure range 0.05–0.30 and total pore volume was determined from the
127 adsorption branch of the N_2 isotherm as the quantity of liquid nitrogen adsorbed at $p/p_0 = 0.995$.
128 Microscopic images were recorded using a Jeol JSM-5600LV scanning electron microscope
129 (SEM). Chemical compositions were determined by X-Ray Fluorescence (XRF) using a Spectro
130 XEPOS instrument with X-LAB Pro software; all measurements were done in He.

131

132 2.6 Catalytic test

133 The esterification reaction of oleic acid with ethanol was performed by reflux in a 500 ml batch
134 reactor placed in a thermostatic oil bath under stirring. The desired amount of catalyst was dried
135 before reaction at 130 °C for 2 h. The reactor was loaded with 50 ml (44.75 g) of oleic acid and
136 the desired amount of pre-heated ethanol (3/1, 6/1 or 9/1 ethanol to oleic acid by molar ratio) was
137 then added. Esterification was carried out over a range of catalyst loadings (2, 5 and 10 wt% with
138 respect to oleic acid) and reaction temperatures (40, 50, 60 and 70 °C). 5 ml samples were
139 withdrawn from the reaction mixture at 15 minute intervals, and centrifuged for 10 min at 3000
140 rpm to separate the solid zeolite from the liquid phase. The supernatant layer was analysed by
141 titration with 0.1 N KOH, using phenolphthalein indicator, to evaluate the acid value (AV) as
142 shown in the following equation;

143

$$144 \quad AV = \frac{\text{ml of KOH} \times N \times 56}{\text{Weigth of Sample}} \quad (1)$$

145

146 From the acid value, the conversion of oleic acid can be calculated for each amount of the catalyst
147 as shown in the following equation;

148

$$149 \quad \text{conversion} = \frac{AV_{t0} - AV_t}{AV_{t0}} \quad (2)$$

150

151 where:

152 AV_{t0} (acid value of the reaction product at time 0)

153 AV_t (acid value of the reaction product at time t)

154

155 The esterification of oleic acid was conducted in the absence of zeolite to determine the extent of
156 any homogeneous reaction. The conversion after 90 minutes was 12% for an ethanol/oleic acid
157 molar ratio 6:1 at 70 °C, showing that while there is some homogeneous contribution the
158 reaction is predominantly due to heterogeneous catalysis by zeolite.

159

160 3. Results and Discussion

161

162 3.1 Catalyst characterization

163
 164 The XRD powder pattern of HY-kaolin is shown in Fig. 1. The three most intense peaks of the
 165 prepared HY-kaolin, located at angles 6.34° , 15.76° and 23.77° 2-theta, confirm the presence of
 166 the characteristic faujasite structure of zeolite Y according to the Commission of the International
 167 Zeolite Association (IZA) [34, 35]. Additional comparison with the corresponding pattern of
 168 commercial HY clearly supports the presence of zeolite Y in the prepared sample, while the
 169 absence of additional peaks in the HY-kaolin pattern confirms that the prepared sample did not
 170 contain any detectable quantity of non-zeolitic crystal phases.

171
 172 Nitrogen adsorption porosimetry results are summarised in Table 1. The BET surface area of the
 173 HY-kaolin, $390 \text{ m}^2/\text{g}$, was lower than that for HY-commercial zeolite, $625 \text{ m}^2/\text{g}$. Similar
 174 differences were observed for the micropore surface areas, A_μ , and micropore volumes, $V_{\mu P}$, of
 175 both samples. When combined with the XRD findings in Fig. 1, the porosimetry results confirm
 176 the presence of micropores in HY-kaolin, whereby the reduced surface area/micropore volume
 177 complements the reduced intensities of the characteristic diffraction peaks. Based on micropore
 178 surface areas, the HY-kaolin contains approximately 65% zeolite Y. The remainder is attributed
 179 to the presence of impurities in the kaolin source, which are not transformed into zeolite and, thus,
 180 contribute to the final product as amorphous, non-zeolitic impurities. The total pore volumes, V_P ,
 181 of both samples are shown for clarity; readings taken close to p_0 will inevitably include intra-
 182 particular condensation, so the higher value attributed to the HY-kaolin (0.853 vs. $0.783 \text{ cm}^3/\text{g}$),
 183 while numerically accurate, is not indicative of the faujasite structure.

184
 185 Table 1: BET adsorption analysis of HY-kaolin and HY-commercial.

Sample	A_{BET} (m^2/g)	A_μ (m^2/g)	V_P (cm^3/g)	$V_{\mu P}$ (cm^3/g)
HY-kaolin	390	235	0.853	0.113
HY-commercial	625	355	0.783	0.258

186 A_{BET} and A_μ are the BET and micropore surface areas, respectively. V_P and $V_{\mu P}$ are the total pore volume (at
 187 relative pressure 0.995) and micropore volume, respectively.

188
 189 Elemental compositions were determined by XRF, Table 2. HY-kaolin contains somewhat
 190 similar amounts of SiO_2 and Al_2O_3 to that in zeolite Y; this is not surprising given that the prepared
 191 sample is predominantly aluminosilicate zeolite Y. The Si/Al ratio of the HY-kaolin was found to

192 be 3.1, which is similar to the value of 2.8 in a similar study using Nigerian Ahoko kaolin [16].
 193 Zeolite X has a Si/Al ratio < 1.5, which means that the more catalytically active and stable form
 194 of faujasite, zeolite Y, is formed here [36]. Major differences in the elemental makeup of the
 195 samples were seen in the relative concentrations of Fe, Na, K, Mg and Ca oxides, which were all
 196 vastly greater in HY-kaolin. These oxides, or various combinations thereof, are hereby assigned
 197 to be the non-zeolitic impurities that are either X-ray amorphous or too dilute to be seen with XRD.

198

199

Table 2: Elemental compositions determined by XRF.

Mass/wt%	Al ₂ O ₃	SiO ₂	Fe ₂ O ₃	Na ₂ O	MgO	K ₂ O	CaO	P ₂ O ₅
HY-kaolin	15.92	58.11	3.191	0.147	1.222	0.067	4.112	0.6448
HY-commercial	13.66	69.74	0.051	0.032	< 0.0034	< 0.0012	0.151	0.5853

200

201 SEM images, Fig. 2, confirm the characteristic micron sized particles of the faujasite structure in
 202 the HY-commercial and the corresponding agglomeration between such particles for the HY-
 203 kaolin samples. It is possible that the impurities in the HY-kaolin have contributed to the
 204 agglomeration in a similar manner to how binders e.g. alumina, are used in the stabilization of bulk
 205 zeolite powders.

206

207 3.2 Esterification reactions

208 The esterification of oleic acid with ethanol is a reversible reaction so an excess quantity of ethanol
 209 is commonly used to enhance conversion. Three ethanol/oleic acid molar ratios were employed;
 210 3/1, 6/1 and 9/1. The fractional conversion of oleic acid, Fig. 3, increases, as expected, with
 211 reaction time and decreases slightly due to catalyst deactivation after 45 min. The conversion is
 212 also found to increase with increasing molar ratio of ethanol to oleic acid; conversions after one
 213 hour were 69% and 85% for ratios 3/1 and 6/1, respectively. There was only a minimal further
 214 increase in conversion for the reaction at 9/1 molar ratio. These results agree with those reported
 215 by SathyaSelvabala et al. who also determined an identical optimum molar ratio of 6:1 in the
 216 esterification of Neem oil using H-mordenite modified with phosphoric acid [37].

217

218 The influence of catalyst loading at oleic acid/ethanol molar ratio of 6/1, Fig. 4, shows an increase
 219 in maximum conversion from 70 to 85% after 60 min going from 2 to 5 wt% but only a small

220 improvement thereafter. A progressive, although slight, decrease in conversion was seen for all
221 catalyst loadings during the second hour of reaction.

222
223 Fig. 5 shows the oleic acid conversion over the temperature range 40-70 °C. The conversion of
224 oleic acid is highly dependent on reaction temperature whereby the maximum conversion increases
225 from approximately 40% at 40 °C to 85% at 70 °C.

226
227 The recyclability of HY-kaolin was examined. Briefly, when the reaction was finished, the catalyst
228 was recovered by filtration, dried at 100 °C, calcined in air at 550 °C for 5 h, and used in a new
229 identical reaction for one hour reaction time. The conversion decreased from 85% to 77%, possibly
230 due to adsorption of water released during esterification, but still retains catalytic activity.

231 232 **3.3 Comparison between HY-kaolin and HY-commercial in esterification reaction**

233 Fig. 6 compares the oleic acid conversion of HY-kaolin with that of the commercially sourced HY
234 zeolite. The difference in activity between zeolites is interesting; the HY-kaolin is somewhat more
235 active in the early stages of reaction, but reduces to the same conversion as the commercial sample
236 after two hours. The difference may be due to impurities in the HY kaolin zeolite which initially
237 enhance the esterification reaction; however, it is difficult to assign such causation with certainty
238 without further exploration and, therefore, this will not be considered further here. Alternatively
239 the effect may be due to the different Si/Al ratios of the sample; 3.1 for HY kaolin versus 4.5 for
240 HY commercial. It is well known that an increase in Si/Al ratio for zeolite Y over the range 2.5-
241 10 causes increases in Bronsted acid strength and catalyst hydrophobicity and a decrease in the
242 acid site density/number [36]. Chung and Park showed that the activities of oleic acid esterification
243 on ZSM-5 and mordenite improved as the number of acid sites increased i.e. with lower Si/Al ratio
244 [38]. A similar increase in activity is observed in this paper for HY-kaolin, which contains a greater
245 number of acid sites than HY commercial, during the early stages of reaction. Chung and Park also
246 reported a conversion of 57% for the same reaction using Y zeolite, Si/Al ratio 3, but did not
247 present any results regarding changes in this ratio. Overall, the findings presented here are in
248 contrast to the claims made in many review papers that microporous zeolites are universally
249 unsuited to the esterification reactions used in biodiesel production, certainly so in the case of oleic
250 acid [5-10].

251

252 **4. Conclusion**

253 Iraqi kaolin was used to prepare Y zeolite in H form. This material was found to be an active
254 catalyst in the esterification of oleic acid with conversion 85% obtained after 60 min reaction time
255 using a 6/1 molar ratio of ethanol/oleic acid at 70 °C. The activity, which was comparable to a
256 commercially sourced zeolite Y, was attributed to a high density of acid sites provided by the low
257 Si/Al ratio (3.1).

258

259 **Acknowledgments**

260

261 ZTA is grateful to the Iraqi Ministry of Higher Education and Scientific Research for financial
262 support to carry out this work at Manchester Metropolitan University, UK, as a part of the
263 requirements for the degree of Doctor of Philosophy in Chemical Engineering at the University of
264 Baghdad.

265

266 **References**

- 267 1. T.M. Albayati, A.M. Doyle, J. Nanopart. Res. (2015) 17:109.
- 268 2. S.P. Singh, D. Singh, Renew. Sust. Energy Rev. 14 (2010) 200–216.
- 269 3. M. Mittelbach, C Remschmidt, Biodiesel, the comprehensive handbook, Boersedruck GmbH,
270 Vienna, 2nd ed. 2004.
- 271 4. M.C. Math, S.P. Kumar, S.V. Chetty, Energy Sust. Dev. 14 (2010) 339-345.
- 272 5. A.F. Lee, J.A. Bennet, J.C. Manayil, K. Wilson, Chem. Soc. Rev. 43 (2014) 7887-7916.
- 273 6. F. Su, Y. Guo, Green Chem. 16 (2014) 2934-2957.
- 274 7. M.K. Lam, K.T. Lee, A.R. Mohamed, Biotech. Adv. 28 (2010) 500-518.
- 275 8. S. Semwal, A.K. Arora, R.P. Badoni, D.K. Tuli, Bioresource Technol. 102 (2011) 2151-2161.
- 276 9. M.E. Borges, L. Diaz, Renew. Sust. Energy Rev. 16 (2012) 2839-2849.
- 277 10. J.A. Melero, J. Iglesias, G. Morales, Green Chem. 11 (2009) 1285-1308.
- 278 11. J. Aracil, M. Martinez, N. Sanchez, A. Corma, Zeolites, 12 (1992) 233-236.
- 279 12. Y. Liu, T.J. Pinnavaia, J. Mater. Chem. 14 (2004) 3416-3420.
- 280 13. C. Belviso, F. Cavalcante, A. Lettino, S. Fiore, 2013. Appl. Clay Sci. 80-81 (2013) 162-168.
- 281 14. S.H. Holmes, A.A. Alomair, A.S. Kovo, RSC Adv. 2 (2012) 11491-11494.
- 282 15. S.H. Holmes, S.H. Khoo, A.S. Kovo, Green Chem. 13 (2011) 1152.

- 283 16. A.S. Kovo, O. Hernandez, S.H. Holmes, J. Mater. Chem. 19 (2009) 6207-6212.
- 284 17. B. Shen, P. Wang, Z. Yi, W. Zhang, X. Tong, Y. Liu, Q. Guo, J. Gao, C. Xu, Energy & Fuels
285 23 (2009) 60-64.
- 286 18. K. Shen, W. Qian, N. Wang, J. Zhang, F. Wei, J. Mater. Chem. A 1 (2013) 3272-3275.
- 287 19. I. Caballero, F.G. Colina, J Costa, Ind. Eng. Chem. Res. 46 (2007) 1029-1038.
- 288 20. G. Wan, A. Duan, Y. Zhang, Z. Zhao, G. Jiang, D. Zhang, Z. Gao, J. Liu, K.H. Chung, Energy
289 & Fuels 23 (2009) 3846-3852.
- 290 21. A. de Lucas, M.A. Uguina, I. Covian, L. Rodriguez, Ind. Eng. Chem. Res. 32 (1993) 1645-
291 1650.
- 292 22. M. Murat, A. Amokrane, J.P. Bastide, L. Montanaro, Clay Mineral. 27 (1992) 119-130.
- 293 23. J. Ramirez-Ortiz, M. Martinez, H. Flores, Front. Chem. Sci. Eng. 6(4) (2012) 403-409.
- 294 24. T.H. Dang, B.-H. Chen, D.-J. Lee, Bioresource Technol. 145 (2013) 175-181.
- 295 25. X. Li, B. Li, J. Xu, Q. Wang, X. Pang, X. Ghao, Z. Zhou, J. Piao, Appl. Caly Sci. 50 (2010)
296 81-86.
- 297 26. L.A.S. do Nascimento, L.M.Z. Tito, R.S. Angelica, C.E.F. da Costa, J.R. Zamian, G.N.
298 RochaFilho, Appl. Cat. B: Environ. 101 (2011) 495-503.
- 299 27. L.A.S. do Nascimento, R.S. Angelica, C.E.F. da Costa, J.R. Zamian, G.N. RochaFilho,
300 Bioresource Technol. 102 (2011) 8314-8317.
- 301 28. L.A.S. do Nascimento, R.S. Angelica, C.E.F. da Costa, J.R. Zamian, G.N. RochaFilho, Appl.
302 Clay Sci. 51 (2011) 267-273.
- 303 29. A.N. de Oliveira, L.R. da Silva Costa, L.H. de Oliveria Pires, L.A.S. do Nascimento, R.S.
304 Angelica, C.E.F. da Costa, J.R. Zamian, G.N. RochaFilho, Fuel 103 (2013) 626-631.
- 305 30. A.H. Mohammed, R.G. Yousuf, K.K. Esgair, Iraqi J. Chem. Petr. Eng. 12(2) (2011) 9-17.
- 306 31. A.H. Mohammed, Z.K. Nassrullah, Iraqi J. Chem. Petr. Eng. 14(1) (2013) 1-13.
- 307 32. J.R. Ugal, K.H. Hassan, I.H. Ali, J. Assoc. Arab Universities Basic Appl. Sci. 9 (2005) 2-5.
- 308 33. A.S. Abbas, R.N. Abbas, Iraqi J. Chem. Petr. Eng. 14(4) (2013) 35-43.
- 309 34. J. B. Parise, D. R. Corbin, L. Abrams and D. E. Cox, Acta. Cryst. C40 (1984) 1493-1497.
- 310 35. M.M.J. Treacy, J.B. Higgins, Collection of Simulated XRD Powder Patterns for Zeolites,
311 Elsevier, Amsterdam, 4th ed. 2001.
- 312 36. J. Weitkamp, Solid State Ionics, 131 (2000) 175-188.

- 313 37. V. SathyaSelvabala, T. K. Varathachary, D. K. Selvaraj, V. Ponnusamy, S. Subramanian,
314 Bioresource Technol. 101 (2010) 5897-5902.
- 315 38. K.-H. Chung, B.G. Park, J. Ind. Eng. Chem. 15 (2000) 388-392.